JOURNAL OF GEOPHYSICAL RESEARCH, VOL. 99, NO. B1, PAGES 577–588, JANUARY 10, 1994

On the electrical nature of the axial melt zone at 13° N on the East Pacific Rise

Rob L. Evans[1] and M. C. Sinha
Bullard Laboratories, Cambridge University, England

S. C. Constable
Institute of Geophysics and Planetary Physics, Scripps Institution of Oceanography, La Jolla, California

M. J. Unsworth[2]
Bullard Laboratories, Cambridge University, England

The first controlled source electromagnetic experiment directly on a ridge, with the potential to identify the presence of an axial melt body beneath a fast-spreading center, was conducted at 13°N on the East Pacific Rise (EPR) in 1989. Transmission for 36 hours was achieved by a deep towed horizontal electric dipole source, of moment 6000 Am, operating at frequencies between 1/4 and 8 Hz. Signals from the source were recorded by seven seafloor electric field receivers positioned both along the ridge crest and 5 km to the east on 100,000-year-old crust. Data above ambient noise levels were obtained at ranges of up to 10 km. The results of modeling observed electric field amplitudes reveal that resistivities in the uppermost crust are very low (~1 Ωm), indicating a heavily fractured, high-porosity surficial layer. Below this topmost layer, the upper 2 km of crust is found to be moderately resistive (~100 Ωm). We find no evidence for a large conductive axial melt body with dimensions on the order of kilometers in the middle or upper crust. If a partial melt body is present, which is continuous along strike and which comprises a connected, and therefore conductive, melt texture, it must be of very limited volumetric extent. This picture is consistent with recently proposed models of a thin sill-like melt lens with across strike dimensions of no more than 1 km and probably with smaller vertical extent. The larger region below the sill, characterized by low seismic velocities, must contain at best a very small melt fraction distributed in isolated pockets, providing further evidence that the EPR at 13°N is currently in a state of relative magmatic quiescence.

Introduction

A consensus seems to have been reached in the mid-ocean ridge academic community regarding ridge-axis melt bodies at midcrustal levels at fast-spreading centers. The paradigm, which is described by a volumetrically small pool of melt flanked and underlain by a larger region of lower melt fraction in a crystalline mush, has come, in particular, from recent interpretations of reflection and refraction seismology [*Kent et al.*, 1990; *Sinton and Detrick*, 1992]. The melt fraction present within the mush zone at any given stage of crustal production remains unconstrained, as do the texture and physical properties of the mush. Two end-member possibilities exist: either melt is periodically injected into the midcrust from the mantle in a single large event, or the melt supply is continuous, but with a smaller melt flux. The constraint on total melt supply is that the observed crustal thickness of about 7 km be produced at the measured spreading rate.

Electrical resistivity models of mid-ocean ridges have traditionally assumed that the melt within the magma chamber forms an electrical conductor: basaltic melt is several orders of magnitude more conductive than dry basaltic rock. The electrical conductivity is, however, highly dependent on the nature of the melt distribution. Complexity of texture will have a dramatic effect on the electrical conductivity of the axial melt zone as a whole and may render these standard electrical paradigms obsolete.

For oceanic crustal studies, controlled source electromagnetic methods (CSEM) are used to measure the large-scale conductivity structure. Accounts and details of the theory and practice of marine EM have been given by *Chave and Cox* [1982], *Cox et al.* [1986], *Constable* [1990], and *Chave et al.* [1992]. An early CSEM experiment by *Young and Cox* [1981], which was conducted 5-15 km from the East Pacific Rise (EPR) at 21°N, ruled out the possibility of the then predicted 20km wide molten magma chamber. The EPR at 13°N (Figure 1) marks the site of the first CSEM sounding to probe the crustal structure of a fast-spreading mid-ocean ridge at the ridge crest. The experiment had

[1] Now at Dept of Physics, University of Toronto, Canada.
[2] Now at Geophysics Program, University of Washington, Seattle.

Copyright 1994 by the American Geophysical Union.

Paper number 93JB02577
0148-0227/94/93JB-02577$05.00

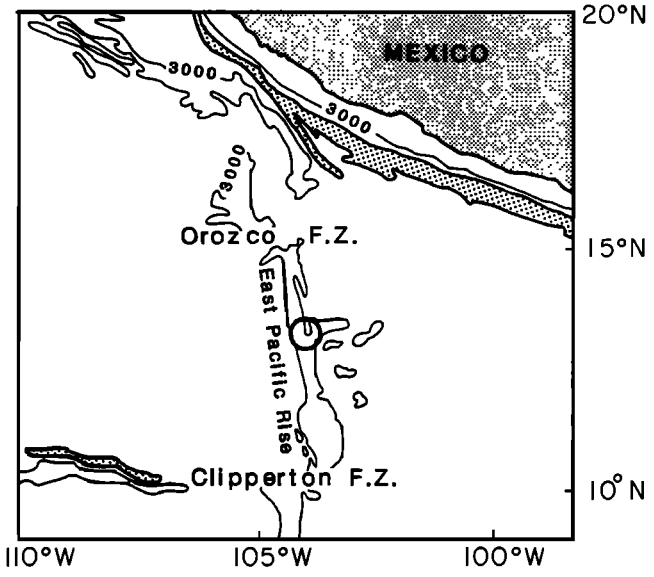

Fig. 1. The location of the experiment site (circle) on the EPR at 13°10′N.

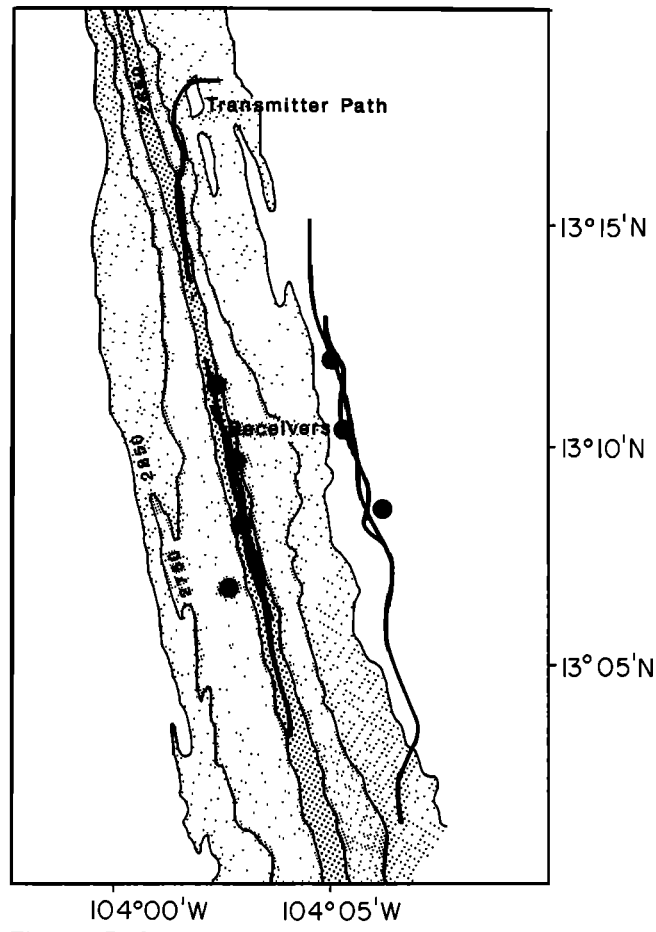

Fig. 2. Bathymetry of the experiment site after *Monti et al.* [1987]. Water depths are in meters. Shown are the positions of the seven receivers (circles). The instruments in each line are spaced approximately 2.5 km apart and the line off-axis is 5 km to the east of the ridge crest on 100,000-year-old crust. The path of the deep tow transmitter during transmission is shown by the solid lines.

the potential to identify the presence of a large conductive anomaly associated with an axial magma chamber. An array of seven remote seafloor electric field receivers measured the signal from a horizontal dipole source over a period of 36 hours. The transmission took place both directly along the ridge crest and on older, 100,000-year-old crust. Signals were recorded above the noise levels, determined from measurements made before and after transmission, to ranges of around 10 km. We have interpreted amplitudes of the seafloor electric field to determine resistivity models of the upper and middle crust. A preliminary account of the resistivity structures in the upper crust (above any possible melt body) has been given by *Evans et al.* [1991]. In this paper, we further examine the data, and in particular address the possible range of resistivity structures in the midcrust representing the expected melt or partial melt zone.

East Pacific Rise at 13°N

The EPR at 13°N (Figure 2) exhibits a roughly triangular cross section. The neovolcanic zone appears to be fairly narrow (~500 m) and flat topped with steep sided flanks which have approximately 100 m of relief [*Monti et al.*, 1987]. The site of our experiment lies on the section of the EPR bounded to the south by the Clipperton transform and to the north by the Orozco transform (Figure 1). More locally, it lies within an extremely linear and bathymetrically two-dimensional segment of the ridge which extends for approximately 90 km between small offsets of the axis at 12°53′N and 13°42′N. With the exception of a minor change in axial linearity (deval) at 13°20′N, the EPR along this segment exhibits very little along strike variability.

On the flanks of the ridge, steep sided grabens run parallel to strike. They are 1-2 km wide, 5-10 km long, and 100-200 m deep and are interpreted to be evidence of normal faulting.

Harding et al. [1989] and *Detrick et al.* [1987] have conducted an extensive seismic survey around this section of the ridge. Their experiment featured a series of expanding spread profiles (ESPs) centered at 13°12′N and a set of multi-channel reflection profiles shot both along and across strike. The along-axis reflection profile shows a weak and irregular event at between 0.5 and 0.6 s two-way time below the seafloor. There is no evidence of a corresponding reflector on any of the cross-axis profiles. Decreases in refracted arrival amplitudes at ranges greater than 11 km along the ridge crest are cited as evidence for a seismic low-velocity zone (LVZ) at a depth of 1.25 km below the seafloor under the ridge axis. The width of the zone is estimated, from ESPs shot parallel to the ridge, to be 4 km or more. Velocities of the model at distances greater than 1 km away from the ridge crest are consistent with rock containing isolated pockets of crystallizing melt. At around 4 km from the ridge the data indicate a normal oceanic crustal structure with no evidence of a LVZ [*Detrick et al.*, 1987]. The region is proposed to consist of a broad chamber, less than 6 km in width, of relatively low melt fraction (less than a few percent) surrounding a 1 km wide by a few hundred meters thick zone of higher melt fraction centered under the ridge crest at a depth of 1.25 km.

Petrological data [*Langmuir et al.*, 1986] from the region are consistent with the magmatic model proposed by seismic studies. Lavas are diverse in composition, even within a single tectonically defined spreading segment, and this is inconsistent with a large, well-mixed chamber.

A detailed gravity survey [*Madsen et al.*, 1990] conducted in this region supports, but does not require, a volumetrically small axial magma chamber. The authors point out that the data are best modeled simply by raising temperatures and allowing thermal expansion of the lower crust and upper mantle at the rise axis. The small density contrast between basaltic melt above and below the solidus makes inference of melt difficult from gravity surveys. Calculated mantle Bouguer anomalies also contain inherent ambiguity regarding their source and can be explained either by anomalous crustal thicknesses, local mantle conditions or crustal density variations.

Based on this evidence, this section of the EPR is often described as having a low magmatic budget, compared to the region around 9°N, where there is strong evidence for ongoing magmatic activity. However, the spreading rate and crustal thicknesses at 13°N are much the same as at 9°N, so that the time-integrated melt flux from the mantle must also be similar. We therefore prefer to describe this ridge segment as being in a period of relative magmatic quiescence.

EFFECT OF MELT ON BULK ELECTRICAL CONDUCTIVITY

Because basaltic melt has an electrical conductivity several orders of magnitude larger than that of the surrounding crystalline rock, its presence can greatly change the total regional conductivity. However, the conductivity depends heavily on the geometry of the melt distribution within the solid matrix. Electrical analogs of ridge structure have, for the purposes of modeling, incorporated a conductive axial melt region a few kilometers in width. This model may be somewhat optimistic since it assumes that the melt fraction throughout this volume (an environment where the melt is cooling and crystallizing) is distributed in an interconnected geometry. This assumption is essential if the partial melt region is to be characterized as a highly conductive anomaly.

Upper, σ^+_{HS}, and lower, σ^-_{HS}, bounds placed on the conductivity of an isotropic two phase medium [*Hashin and Shtrikman*, 1962; *Waff and Weill*, 1975; *Schmeling*, 1986] account for the two limiting cases of complete fluid interconnection and of isolation:

$$\sigma^-_{HS} = \sigma_o + \beta\left((\sigma_1 - \sigma_o)^{-1} + \frac{(1-\beta)}{3\sigma_o}\right)^{-1},$$

$$\sigma^+_{HS} = \sigma_1 + (1-\beta)\left((\sigma_o - \sigma_1)^{-1} + \frac{\beta}{3\sigma_1}\right)^{-1} \quad (1)$$

where σ_o is the rock conductivity, σ_1 is that of the conductive fluid phase, and β is the melt fraction. If the two-phase system is in textural equilibrium, as it is under mantle conditions [*Cheadle*, 1989], then the lower, least conductive limit, relating to an unconnected melt distribution, will apply where the dihedral angle between grain boundaries is greater than 60°. In this case, the melt phase is distributed in isolated pockets, and ionic charge carriers are unable to propagate between inclusions. The bulk conductivity will be dominated by the crystalline phase. If, on the other hand, the system has values of dihedral angle less than 60°, the melt will form a connected network. Here, conduction can occur between grain boundaries via the melt, and the conductivity will be greatly enhanced. Where the dihedral angle is zero, which is actually rarely observed, all grain boundaries will be wetted. It is believed that basaltic melt always forms interconnected networks in mantle rocks. However, the upper Hashin-Shtrikman (HS) bound strictly applies only in the case of complete wetting and for that reason yields conductivities which are probably higher than we may expect to measure. At surface levels, where the melt is crystallizing, the crust may undergo brittle failure, and the distribution of fluid-filled cracks will be far more important to the conduction mechanism than grain boundary geometries. The crust and melt are unlikely to be in textural equilibrium and the models used to describe mantle melt distributions are inapplicable. Furthermore, the strongly oriented tectonic stresses increase the probability of anisotropy within the the melt zone, further complicating the electrical structure.

Schmeling [1986] has described intermediate scenarios where the conductive phase occurs in spheroidal inclusions of various aspect ratios. For a given crack density and melt fraction it is the shape of inclusion that dominates the conductivity: narrow cracks increase the probability of one or more connected pathways through the solid. At small (less than 1%) crack densities and melt fractions, however, under almost any melt geometry, conduction is controlled by the solid country rock.

One of the few direct observations we have of igneous structures in what was once a mid-ocean ridge crustal magma chamber has come from Ocean Drilling Project (ODP) hole 735B, drilled during leg 118 on the SW Indian Ridge [*Dick et al.*, 1991]. Although the tectonic setting of this environment is one of very slow spreading, the textures observed may well be relevant to the types of melt distribution likely to be found at the extremities of the melt zone, even at fast spreading segments. The crust at 735B is described as having undergone "syntectonic differentiation," in which late melt injections are intruded into cracks formed by the brittle failure of existing rock under tectonic stresses. Late melt injections into the sequence, which are thought to have occurred a short distance from the ridge crest, seem to have been intruded into isolated veins and cracks formed from the brittle-ductile failure of the gabbros. Intrusions cover several scales, from cross-cutting igneous dykes to small intrusive microgabbros. These data seem to indicate that the electrical resistivity throughout an axial melt zone, even at fast spreading ridges, will increase with distance from the ridge crest as the melt fraction decreases due to cooling of the surrounding host, and the size and number of intrusive veins containing melt decreases. Such a texture is far removed from traditional views of crystal settling magmatic processes, of which there is almost no evidence in hole 735B, and which may only occur after a fresh injection of mantle-derived melt into the crust.

In general, as far as magma bodies are concerned, the presence of melt is a necessary, but not sufficient, condition for a conductive anomaly. Under the tectonic conditions described, regions of the crust with a few percent unconnected melt fraction would have a bulk electrical conductivity dominated by the crystalline phase. However, since constraints on the texture of melt distributions are as important in determining the behaviour of the magmatic phase as those on the melt fraction itself, CSEM experiments provide important information which is complementary to that derived from seismic and other methods, even in the absence of a conductive anomaly.

SENSITIVITY OF MARINE EM DATA TO BURIED CONDUCTORS

CSEM soundings require the deployment of a series of remote seafloor receivers which measure the signal from a transmitting source which is towed close to the seafloor. In the vicinity of the ridge, two possible configurations of source and receivers which take advantage of the symmetry of the ridge can be envisaged. One arrangement, which will be referred to as the "1-D experiment," is where the receivers are placed in lines parallel to strike and the transmitter is towed along these lines. If the ridge structure is invariant along-strike, or two-dimensional (2-D), the resistivity below the transmitter will be the same at all points on a given tow line. The other configuration involves transmission perpendicular to strike, across the ridge crest. In the presence of an axial melt zone (AMZ) this experiment would incur significant changes in structure beneath the profile. Transmission across strike would almost certainly require attention to 2-D effects and will be referred to as the "2-D experiment."

Before we include certain generic geological features in our models, we should determine which parts of the data set are most sensitive to their presence. One of the features of most interest in the analysis we have undertaken is the AMZ which, ideally, would constitute a conductive target within the crust. A conductive "end-member" case would occur if the texture of the region containing melt satisfied the condition for the upper HS bound. If we assume a modest melt fraction, say 10%, then such a melt zone would have a low resistivity around 3 Ωm.

The resistivity of the overlying crust is dominated by the penetration of seawater, and increases monotonically to values of around 100 Ωm at a depth immediately above the top of the LVZ. If the LVZ is indeed conductive, there would be a significant contrast in conductivity over a relatively small vertical distance. At the other extreme, if the melt were in isolated pockets, a resistive end-member might be imagined where the resistivity structure would not be significantly altered by the presence of melt fractions even as high as 30%.

There are several problems of resolution in the 1-D experiment which lead to difficulties in requiring the existence of a conductive body from incomplete and error-bound data. What constitutes a conductor is, in practice, very dependent on the frequency of transmission and on the size of the anomaly. The frequencies used for CSEM experiments are chosen so that the electromagnetic skin depths within the crust are on the same order as the source-receiver separations. The electromagnetic skin depth, δ, measured in meters, describes the length scale over which the electric fields at a particular frequency, f, decay. It is given by

$$\delta = 503\sqrt{\frac{1}{f\sigma}}, \tag{2}$$

where σ is the conductivity of the medium in which the fields are propagating. Low frequencies such as those available for oceanic magnetotelluric soundings have periods of a few minutes upwards and are almost completely insensitive to crustal melt distributions. On the other hand, if the frequencies used are too high, the skin depths in the crust will be very short and the transmitted fields will be rapidly attenuated below measurable levels.

Model Studies Using Regularized Inversion

A first approach to estimating sensitivity to buried conductors is to assume that the seafloor conductivity changes as a function of depth only. The algorithm of *Chave* [1983] was used to calculate the electric fields of a dipole source over a layered Earth. The theory for the calculation is given by *Chave and Cox* [1982].

Forward modeling shows that the effect of a conductive layer at depths of 1 to 1.5 km is to enhance amplitudes at intermediate ranges (3-6 km) and to rapidly attenuate the amplitude at longer ranges. The enhancement is due to the entrapment of fields in the resistive layer between the seawater and melt in what has been called a "quasi-waveguide" effect [*Chave et al.*, 1990]. The rapid attenuation at long ranges indicates penetration and loss of energy into the conductive body.

We have calculated synthetic data sets for a model which includes a 200-m-thick conductive layer, representing a melt layer, underlain by a region representing ~5% interconnected partial melt (Figure 3). The resistivity structure in the upper crust above this is based on the results of *Evans et al.* [1991]. Two frequencies, which are the highest and lowest transmitted in the EPR experiment, have been considered, 8 Hz and 1/4 Hz. A series of synthetic amplitudes have been generated for each.

We shall consider first the results of inverting 8-Hz synthetic amplitudes only. Before inversion, the synthetic amplitudes were distorted by varying degrees of noise. Smooth models were derived by inversion from the noise-distorted synthetic amplitudes, using the routine of *Constable et al.* [1987]. The models derived all have a response which fits to the expected rms misfit of 1.0. The misfit is defined in a standard least squares sense as

$$X^2 = \sum_{i=1}^{M}\left[\frac{(d_i - F_i[m])^2}{\epsilon_i^2}\right], \tag{3}$$

where d_i are the M synthetic data points and $F_i[m]$ are the corresponding predicted reponses from the preferred model, m. The misfit is normalized by standard errors, ϵ_i, derived from the added noise.

The 8-Hz synthetic amplitudes were inverted and a discontinuity was allowed at 1 km, the onset of the conductive region predicted by seismic reflection data. In the first case, the added noise was representative of errors and scatter obtained during our experiment on the EPR (Figure 3) and give errors of about 15-20% [*Evans et al.*, 1991]. From the results, it is clear that 8-Hz data with range content of less than 8 km and these large-amplitude errors are not able to describe the starting model with the conductive zone accurately. This result remains true even when smaller, centrally distributed errors of 5% were applied, and the range extended to 12 km. However, the structure of the model above the conductor was returned in all the synthetic inversions.

The inclusion of 1/4-Hz synthetic data in the inversion yields a solution that is closer to the original model. The two synthetic data sets had centrally distributed errors of 15% in amplitude applied. The values obtained at both frequencies were then simultaneously inverted (Figure 4). The resulting solution contains the general form of the starting model, characterized by a downturn in resistivity at a depth

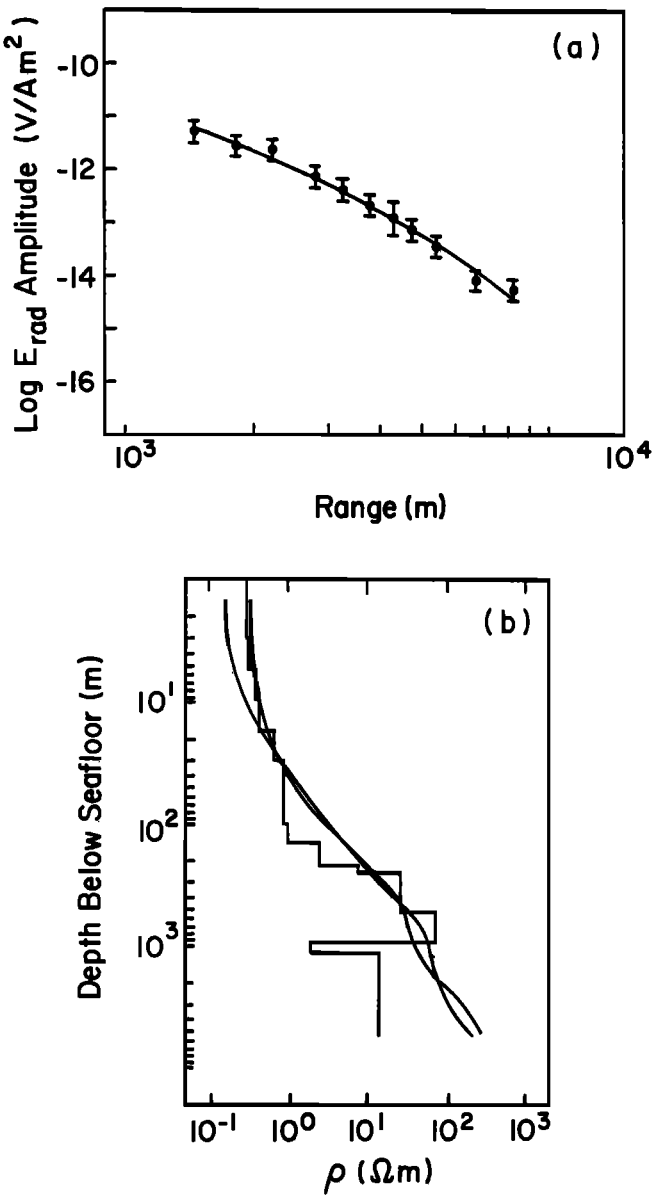

Fig. 3. Inversion of 8-Hz synthetic data generated from the layered model shown in Figure 3*b*. The conductive layers below 1 km are representative of a thin layer of high melt fraction overlying a region containing about 5% melt fraction. The synthetic data are shown in Figure 3*a* and were truncated at the longest range at which 8-Hz data were measurable during the EPR experiment. Errors of similar magnitude to those observed (15-20%) were also applied to the synthetic data. The smooth model shown in Figure 3*b* is the result of inverting this synthetic data with a response which is shown as the solid line in Figure 3*a* and which fits to rms 1.0 (see text).

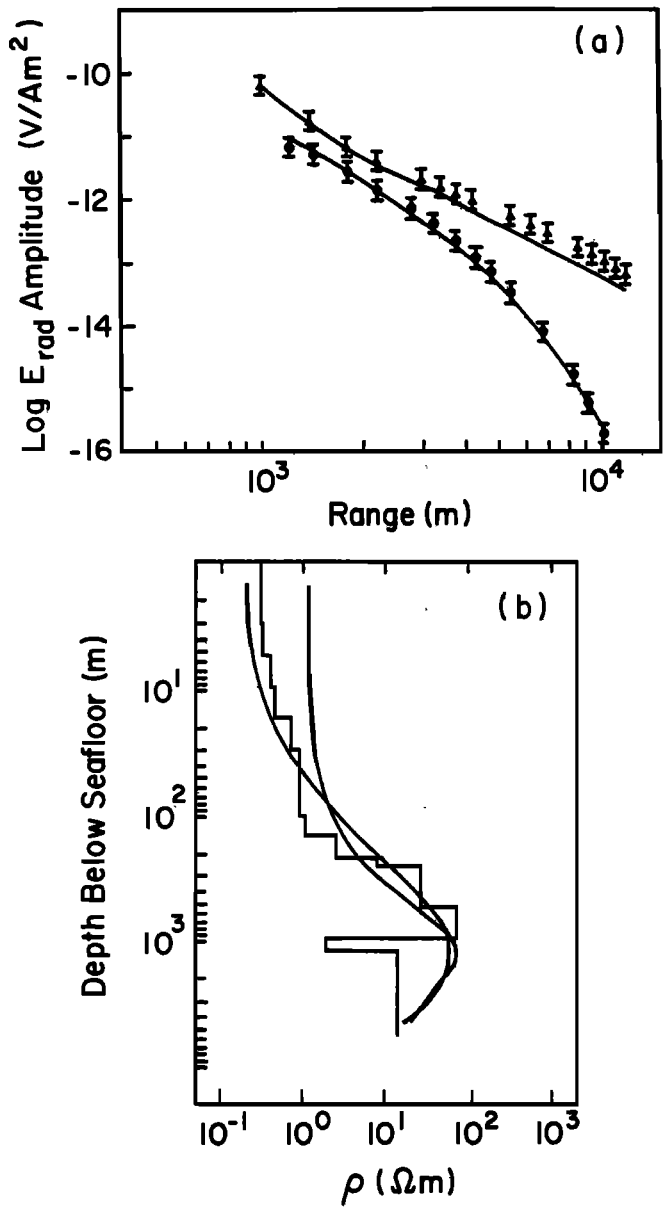

Fig. 4. The simultaneous inversion of both 8-Hz and 1/4-Hz synthetic data, generated by the same layered model as in Figure 3 and also shown in Figure 4*b*. The data generated are shown in Figure 4*a* with the circles used for 8-Hz amplitudes and triangles for the 1/4-Hz values. Data coverage has been extended to a range of 12 km, and errors of 15% applied. Two models which are smoothed in a first and second derivative sense were obtained which both contain a downturn in resistivity at around the same depth as the buried conductive layers. The result indicates the sensitivity of a combination of 8-Hz and 1/4-Hz data to the presence of a buried conductive layer.

around 1 km. These results demonstrate the greater degree of sensitivity of data at 1/4 Hz to the presence of a conductive layer typical of basaltic melt. We can therefore conclude that a combination of 1/4 Hz and 8 Hz data of comparable quality to those obtained in our experiment is sensitive to the presence of a buried conductive layer, and to the resistivity structure above it. Other means of evaluating sensitivity, such as singular value decomposition and analysis of Fréchet derivatives [*Chave*, 1984], also concur with this conclusion [*Evans*, 1991].

Two-Dimensional Effects

Mid-ocean ridges are clearly not 1-D features, and their electrical structure may be expected to vary across and along strike in addition to changes with depth. The inversion of data collected during our experiment is restricted to a 1-D parameterisation, as 2-D controlled-source inversion schemes are currently unavailable. It is important therefore to understand the characteristic responses of 2-D features so that, if necessary, they can be identified in the data.

In terms of electromagnetic sounding, the effect of a buried conductor in a layered, resistive Earth depends on the experimental geometry. Transmission across strike has been dealt with numerically by *Everett and Edwards* [1991] and by *Unsworth* [1991; *Unsworth et al.*, 1993], and we will not further discuss this scenario.

Transmission along strike corresponds to the geometric arrangement adopted during the experiment on the EPR we are describing. The response of a buried conductor will differ from the 1-D solution when the width of the body is narrowed below a critical width which is dependent on the frequency and on the conductance of the body (conductance is defined as the conductivity of the body times some appropriate scale length). The width of conductor needed for the 1-D assumption to be valid increases with decreasing frequency, while the "waveguide effect" is greater for lower frequencies. The presence of 2-D variations in conductivity leads to questions of how good an approximation is the assumption of a layered Earth locally beneath the transmitter-receiver line and which geometries of melt, if any, yield responses distinguishable from a 1-D response.

We have examined some of these issues by carrying out 2-D forward modeling. In our 2-D models, a background electrical structure based on the upper crustal model of *Evans et al.* [1991] has had superimposed on it a conductive body of infinite along strike length, and a vertical thickness of 500 m, situated at a depth of 1.2 km beneath the ridge crest to coincide with the seismic low velocity zone measured by *Harding et al.* [1989]. The width of the conductive prism is varied, and the shift in response from that of the background resistive structure is calculated using the finite element code of *Unsworth* [1991; *Unsworth et al.*, 1993]. Again we have considered two frequencies, 8 Hz and 1/4 Hz. Figure 5 shows the shift in the electric field amplitude for a layered Earth containing the conductive body described above, relative to the response of the layered structure without the body. The source-receiver separation is 7 km, which is approximately where the largest amplitude enhancement is seen in the layered models we have considered. Figure 5 shows four curves, two for each frequency, which consider a body of effectively pure melt of resistivity 0.25 Ωm and one of moderate melt fraction, 2 Ωm.

At 8 Hz, bodies wider than ~5 km have a predicted 2-D response which is experimentally indistinguishable from that of an infinitely wide layer. Smaller bodies pose more difficulty, however, as they trap currents from the sides as well as from above. As the body is narrowed below 5 km, an optimal width is reached where the channeling is most efficient. For the more conductive body considered, at widths above approximately 1 km, the field is significantly enhanced even above that resulting from a conductive 1-D layer. This further enhancement is greater for more conductive bodies and for the lower frequency considered (1/4 Hz). At widths below about 1 km the channeling becomes less efficient as the body becomes electrically small. The response then asymptotes towards that expected from the purely resistive layered Earth. However, the results of the modeling demonstrate that the presence of a 2-D conductive body beneath the line of transmission always enhances amplitudes above the response of the resistive Earth with no conductive anomaly, at least over the ranges to which we have recorded data.

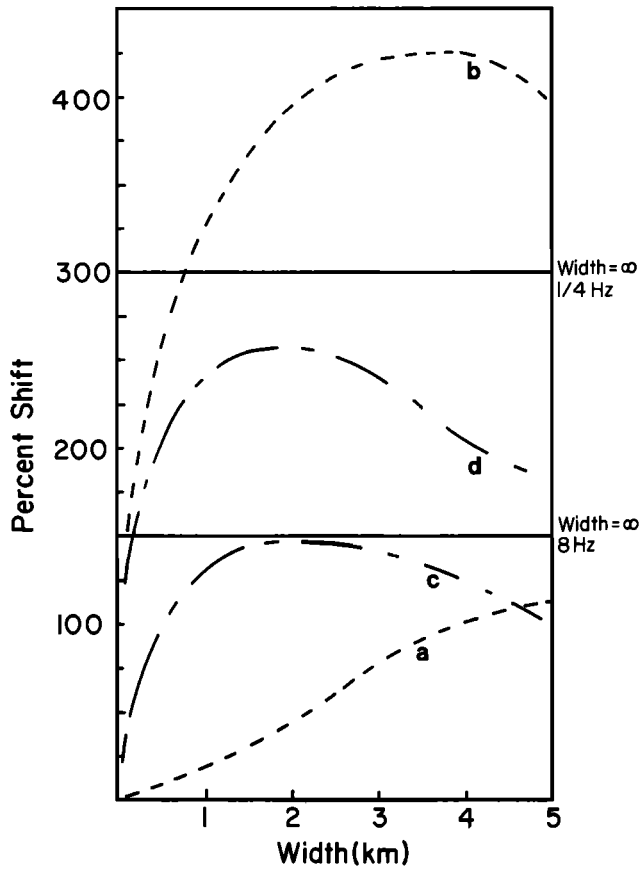

Fig. 5. The results of modeling a 2-D conductivity structure containing a rectangular conductive body buried at a depth of 1.2 km and of 500-m thickness. The width of the body was changed, and the percentage shift in the electric field relative to the response without the body calculated. Two bodies were considered: a pure melt body of resistivity 0.25 Ωm, and a partial melt body of resistivity 2 Ωm. Two transmission frequencies were also considered (see text for discussion): 8 Hz and 1/4 Hz. Curve a is for 1/4-Hz transmission and a body of 2 Ωm, curve b is for 1/4-Hz transmission and a body of 0.25 Ωm, curve c is for 8-Hz transmission and a body of 2 Ωm, and curve d is for 8-Hz transmission and a body of 0.25 Ωm. The presence of a conductive body always enhances amplitudes above the response to the same 1-D model without a conductive layer at the same source-receiver separation. Narrow bodies are less efficient current channels and their response is correspondingly close to the resistive limit. The response of an infinitely wide body of resistivity 0.25 Ωm is shown for each frequency.

EXPERIMENTAL PROCEDURE

The sounding experiment described in this paper took place in June 1989 over a period of 8 days on station at 13°N (Figure 1) on the EPR.

The transmitting source consists of a 100-m horizontal electric dipole of moment 6000 Am, which is part of a neutrally buoyant streamer [*Sinha et al.*, 1990]. The streamer is attached to a deep tow, which is flown at heights of the order of 30 m above the seafloor. The penalty incurred by flying at this height is a reduction in the amount of energy diffusing into the seabed, although it allows transmission directly over the ridge crest where the topography is rough and could cause damage to a transmitter placed on the sea floor. An in-phase stacking procedure is employed by the

receivers to reduce the volume of data, and so it is important to maintain as constant a height as possible in order to minimize phase variations in the received signal. The height above the seafloor is monitored by an echo sounder mounted on the front of the deep tow package and is controlled by paying out or hauling in wire. During the final two lines, excellent stability in the deep tow height above the seafloor was obtained with variations in height of less than ±10 m over a 15-min interval during which typical heights above the seafloor of 30 m were attained. A 10-m shift in height at 8-Hz transmission would change the electric field phase by about 6° and the amplitude by about 10%.

The receivers are independent packages utilizing 12-m electric antennae to measure the horizontal electric field at the seafloor [*Sinha et al.*, 1990; *Webb et al.*, 1985]. Each has an orthogonal pair of dipoles equipped with low noise Ag-AgCl electrodes based on the design by *Filloux* [1987].

Receivers were deployed in two strike-parallel lines; one along the ridge crest, with four instruments placed ~2.5 km apart and the other, of three instruments, ~5 km to the east and parallel to strike on 100,000 year old crust (Figure 2). The lines along which the transmitter was towed and the siting of receivers were designed to facilitate and to optimize a 1-D interpretation of the data: transmission was parallel to strike and signal was received on a co-linear series of receivers.

Unfortunately, almost two thirds of the planned experiment time was lost due largely to an unstable political situation in Panama, the initial port of call. This loss of time meant that a limited transmission period of only 36 hours was available once the receivers were in place, and prevented any attempt at an across-strike survey.

Before starting the CSEM work, an array of six acoustic transponders was deployed around the experiment site to provide precise real-time navigation throughout the area. A relay transponder was attached to the deep tow cable, making it possible to provide accurate information of both the ship and deep tow package positions relative to the seafloor. The system was tied into Global Positioning System (GPS) satellite coverage in order to relate relative positions to global coordinates.

Tow lines were approximately 9 km long and took 4-5 hours to complete at speeds of around 1 knot (1.85 km h^{-1}). Additional time was spent in turning the transmitter onto the adjacent line. Initial transmission, both along the ridge crest and along the strike-parallel line, 5 km to the east, consisted of 15-min blocks per frequency for six different frequencies; 1/4, 1/2, 1, 2, 4, and 8 Hz. Final tow lines, featuring continuous 8-Hz coverage, were then completed both on and off axis. At 8 Hz the skin depth in seawater is 100 m. The next frequency offered by our system is 16 Hz, at which the height of the transmitter above the seafloor is a significant fraction of the skin depth. For this reason, 8 Hz was chosen to be the highest frequency transmitted. At 1/4 Hz the typical crustal skin depths are about 10 km, which is the length scale of the experiment, and so this was chosen to be the lowest transmitted frequency.

APPROACH TO DATA REDUCTION

The seafloor electric field is recorded in stacked time series. These sequences are passed through a Fast Fourier Transform (FFT) routine, and the spectral components corresponding to the frequencies of transmission are examined. Transmission frequencies are precisely on the center of the FFT bins so that windowing is neither necessary nor desired.

The data recorded before and after transmission, as well as data recorded during breaks in transmission, are used to determine the ambient noise levels. Noise levels vary between instruments but are typically 10^{-15} VA^{-1} m^{-2} in a bandwidth of 10^{-3} Hz at 8 Hz, or, normalized to the frequency bandwidth, 10^{-19} V^2 m^{-2} Hz^{-1}. This value serves to cut off data recorded, at 8 Hz, at a range of ~8 km.

The electric field measured by each pair of orthogonal electrodes is recorded simultaneously on separate channels. These data are combined geometrically into components radial to, and azimuthal to, the transmitter-receiver direction. The geometric information required to complete the decomposition is obtained from the complete navigation coverage obtained throughout the sounding and from compass readings inside the receivers which give the orientation of the dipole arms on the seafloor. During transmission the source was parallel to strike. Since the electric field measured in this direction has only a radial component, *Evans et al.* [1991] chose to model the radial component of horizontal electric field, E_{rad}. Another decomposition, in terms of the polarization ellipse of the seafloor electric field, is possible, and details are given by *Smith and Ward* [1974]. The amplitude of the major axis of the ellipse, E_{maj}, depends only on the amplitudes measured on the two orthogonal receiver channels and on the relative phase difference between the signals. Therefore geometric dependence is largely removed from the data which helps to reduce the scatter in observed amplitudes due to effects other than surface heterogeneity. Amplitude data are also normalized to zero transmitter height by a simple skin depth factor, before modeling and inversion.

The complete set of amplitudes collected during the experiment is shown in Figure 6, separated into the different frequencies transmitted. Data collected along the ridge crest are shown as triangles, and those collected on 100,000-year-old crust as circles.

DATA INVERSION

Amplitudes of the seafloor electric field, at each frequency of transmission and at all available source-receiver separations, have been modeled using the inversion routine of *Constable et al.* [1987]. The algorithm seeks optimally smooth models that fit the data to the expected degree of misfit, with resistivity a function of depth only ($\rho = \rho(z)$). The philosophy of searching for optimally smooth models, especially when modeling potential field measurements, has been widely documented and discussed [e.g., *Parker*, 1980, 1984]. By finding the models which have the minimum amount of structure required to satisfy the data, we simultaneously find the maximum amount of structure which we can reliably infer from our experiment alone. Other a priori information can then be included in careful modeling, once the resolution of the sounding to such features is established.

The smoothness of a discrete model of N layers is defined either in the first or second derivative sense. Penalizing roughness with respect to the first model derivative seeks the flattest model possible, or the model closest to a

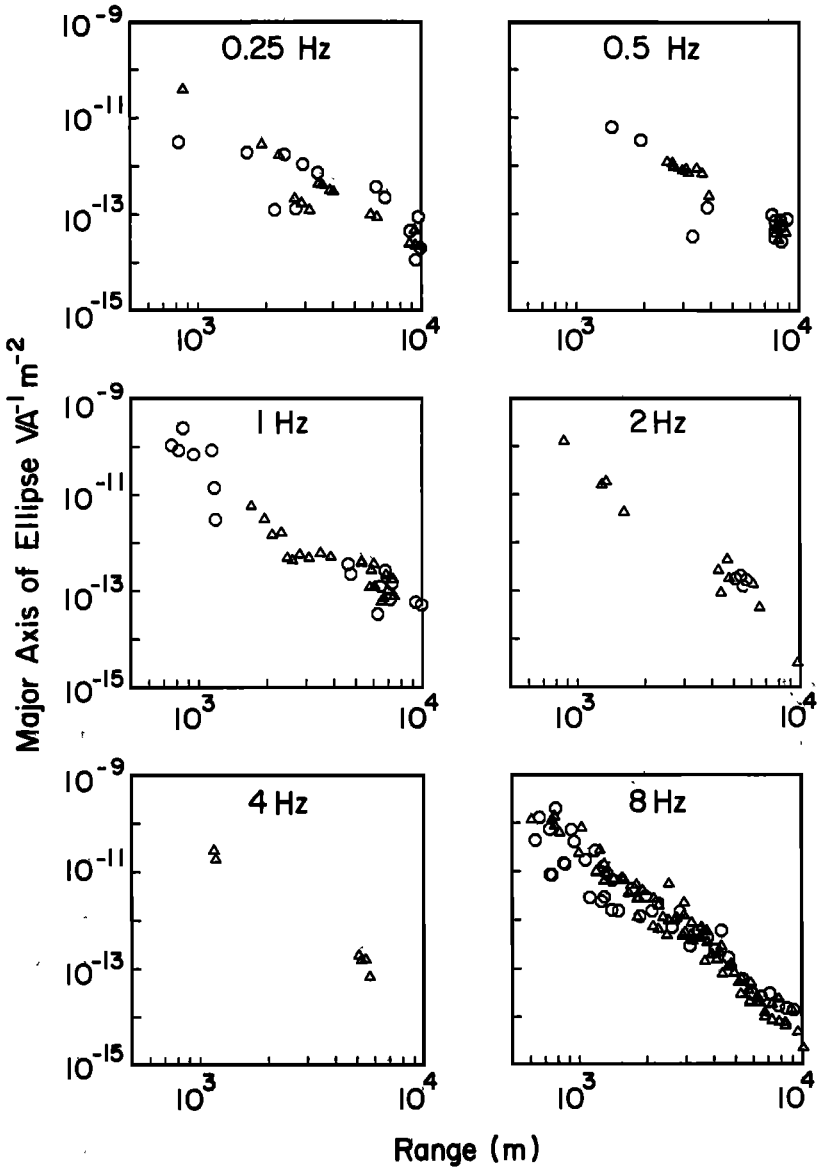

Fig. 6. The entire data set collected at each transmission frequency, expressed as the amplitude of the major axis of polarization ellipse, E_{maj} (see text). Data collected along the ridge crest are denoted by triangles and those collected 5 km to the east of the ridge crest by circles. Note the similarity between the two groups.

uniform half space. Penalizing roughness with respect to the second model derivative finds the least oscillatory or "wiggly" model. In the absence of a priori information, smooth models are appropriate for electromagnetic induction which is, by nature, diffusive and smears out sharp boundaries or interfaces. The misfit is normalized by standard errors in the data, ϵ_i, in equation (3), which are calculated by averaging amplitudes collected at similar ranges. Means and standard errors in the means are calculated in the log-amplitude domain for the data in each range bin. By averaging, we hope to generate objective errors which account for the large degree of scatter observed in values, and which is believed to be caused by surface heterogeneity in the resistivity structure. We aim for an rms misfit of 1.0 in all cases.

MODELING OF EPR 8 HZ DATA

The 8-Hz amplitude data collected during the experiment make up the most comprehensive and consistent subset of the data. The decrease in amplitude with range follows an expected pattern, but cannot be explained by a simple half-space model, illustrating the fact that we have sampled regions of varying structure with depth [*Evans et al.*, 1991].

Amplitude data from along the ridge crest and from the parallel line have been partitioned into range bins, as has been described previously [*Evans et al.*, 1991]. The two populations, on and off axis, are virtually identical [*Evans et al.*, 1991]. Scatter in the data is observed in both lines, which is thought to be largely caused by surface heterogeneity.

The regularized inversion of both E_{rad} [*Evans et al.*, 1991] and E_{maj} data sets collected on and off axis produces almost identical models, in the first and second derivative sense, with resistivity increasing monotonically with depth. These models are shown in *Evans et al.* [1991]. The E_{maj} data sets are less scattered than their E_{rad} counterparts because this decomposition eliminates errors in transmitter azimuth. Smooth models arising from the inversion of the binned data set collected along the ridge crest are shown

in Figure 7*b* for both an E_{maj} and an E_{rad} decomposition. Divergence points between the first and second derivative smooth models for each of the two data sets indicate loss of resolution in the data at depths shallower than ~50 m and deeper than ~1 km below the seafloor. Resistivity increases from approximately 1 Ωm at a depth of 50 m, to around 90 Ωm at 1 km.

MODELING OF LOWER FREQUENCY EPR DATA

Largely because of the short time available for transmission, the lower frequency data collected during the cruise were less extensive than that at 8 Hz. This makes binning of data to obtain acceptable error estimates difficult or even unreliable. However, it is clear upon examining the lower frequency amplitudes obtained that we are still able to draw conclusions about the acceptable classes of model solution.

We have used the 8-Hz result to model the lower frequency data. In this way, having constrained the upper crust, we have examined whether melt bodies are compatible with the data. The model obtained from 8-Hz data has a response which predicts slightly higher amplitudes (~10%) than are seen by 1/4-Hz and 1/2-Hz data (Figure 8). However, the density of the lower frequency data is not sufficient to exclude the 8-Hz model. What is clear from these data, however, is that we cannot include a wide conductive body in our model and fit all our data simultaneously: the 1/4-Hz and 1/2-Hz data do not exhibit the enhancement in amplitude characteristic of such features. The response of the model containing a conductive layer below 1-km depth, which satisfies 8-Hz amplitudes [*Evans et al.*, 1991], clearly does not fit the lower frequencies (Figure 8).

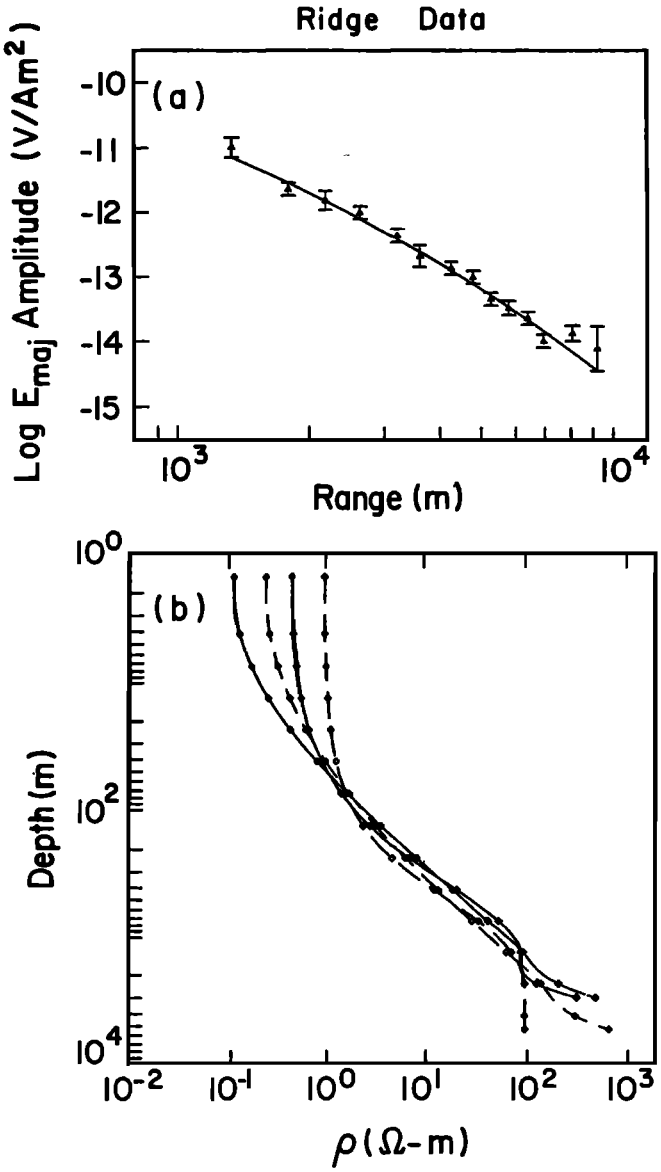

Fig. 7. (*a*) The binned 8-Hz data collected along the rise axis decomposed into the amplitude of the major axis of polarization ellipse, E_{maj}. The solid line is the response of our preferred smooth models. (*b*) The two optimally smooth models in a first and second derivative sense for the binned E_{maj} (solid curves) data. Shown also (dashed curves) are the the results for inverting the data as an E_{rad} decomposition.

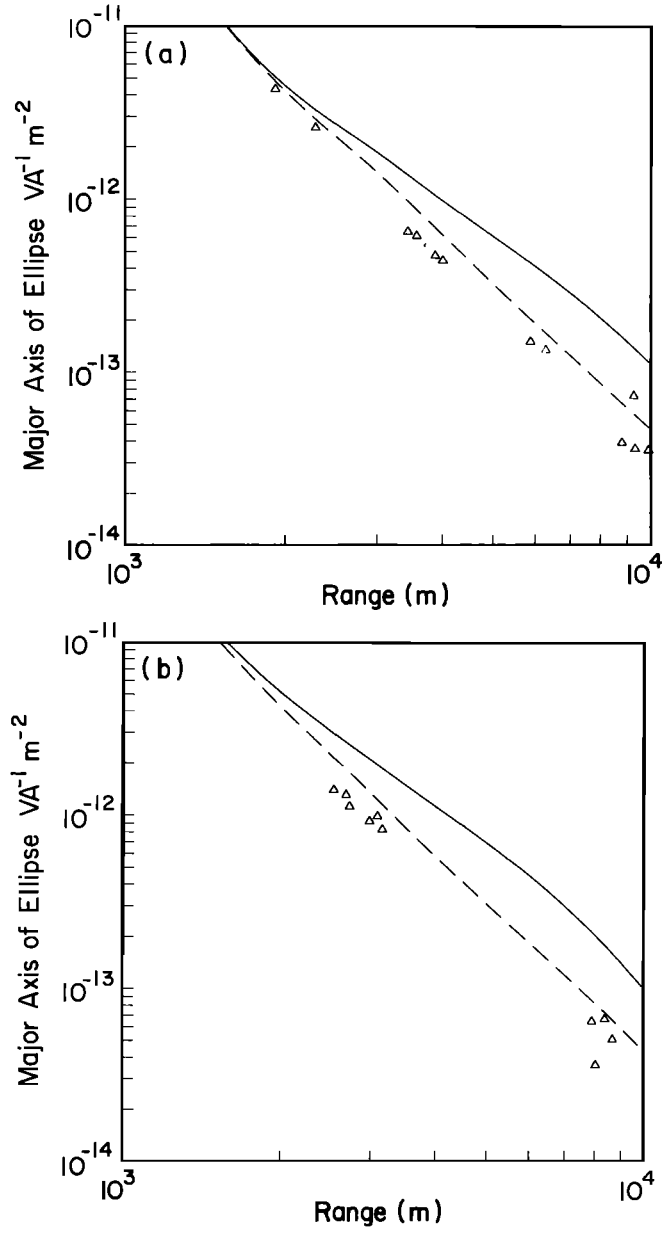

Fig. 8. (*a*) The 1/4-Hz data collected along the ridge crest. The dashed line is the response, at 1/4 Hz, of the smooth model obtained from inversion of 8-Hz amplitude data. The solid line is the response of the 8-Hz model underlain by a conductive termination at a depth of 1.2 km. (b) The same as Figure 8*a* for the 1/2-Hz data collected along the ridge crest.

Two-dimensional modeling studies allow us to define exactly what we mean by a wide conductive body in this scenario and to place limits on the size of melt body that could have been resolved. A body of resistivity around 5 Ωm but of width less than ~1 km, centered at the ridge axis, will not greatly enhance amplitudes above the resistive solution at 1/4 Hz. A resistivity of 5 Ωm corresponds to a connected melt fraction of ~7%. Higher melt fractions could remain undetected if they lie in isolated pockets.

Two-dimensional parameterisations themselves involve the limitation that a conductive body possesses infinite length along strike. This may also be a severe limitation in the modeling of along-strike field data by such techniques. Petrological [*Langmuir et al.*, 1986] and ophiolite studies [*Browning*, 1984; *Malpas*, 1990] have provided convincing evidence that large, well-mixed, axial magma chambers are incompatible with the diversity of chemical compositions recovered, and that large-scale melt migration along strike is unlikely to occur beyond the limits of a tectonically defined spreading cell. Seismic reflection profiles gathered in this area highlight the discontinuous nature of pockets of large melt fraction that are typically modeled as 2-D. Once a conductive body becomes finite in all dimensions, on similar length scales to the source-receiver separation, current channeling effects will result in different characteristic responses. Buried three-dimensional bodies have weaker responses and are notoriously difficult to detect. Attenuation of the field may be seen in an along-strike experiment, in much the same way as for the trans-ridge sounding [*Unsworth*, 1991; *Unsworth et al.*, 1993; *Everett and Edwards*, 1991]. That the low 1/4-Hz and 1/2-Hz amplitudes observed in this experiment may be due to such effects should not be discounted.

TECTONIC IMPLICATIONS

The uppermost 150 m, or so, of crust is required to be heavily fractured in order to explain the low resistivities derived from our 8 Hz amplitude data. In the uppermost crust, the seismic models of *Harding et al.* [1989] and *Detrick et al.* [1987] are consistent with our interpretation of a heavily fractured uppermost layer, with inferred porosities of around 20%, which is underlain by a sharp gradient in physical properties, interpreted as a rapid decrease in bulk porosity and, hence, fluid content. The similarity of 8-Hz data collected along the ridge crest and on 100,000-year-old crust indicates a similarity in bulk structure between the two crustal ages. There is no evidence for a thickening of the uppermost layer of extrusives away from the ridge crest. If the thickening of seismic layer 2A seen at 9°N on the EPR is due to volcanic flows away from the ridge crest [*Christeson et al.*, 1992], then the EPR at 13°N seems to have exhibited only modest volcanism over the last 100,000 years. The large degree of scatter observed in amplitudes, both on and off axis, is likely to indicate surface heterogeneity. Unfractured sheet flows, near-surface dyke intrusions, and fissures may be the source of this heterogeneity.

Beneath the ridge crest, the proportion of melt which is sufficient to produce an intracrustal AMZ reflector, where it is seen, will almost certainly be associated with an increase in electrical conductivity. However, it is unclear whether the region of low velocities below, and to the sides of this reflector will be electrically conductive. An ESP 1.5 km from the ridge crest at 13°N requires only a thin (~300 m) LVZ in which velocities are depressed from ~6 km s^{-1} to around 5 km s^{-1}, although it should be borne in mind that the velocity structure within a LVZ is poorly constrained by wide-angle seismic data. Such a reduction in velocity may correspond to a small melt fraction which is undergoing crystallization and which may not exist within an interconnected network.

The theoretical results of *Kuster and Toksoz* [1974] show that for low porosities and, hence, noninteracting inclusions, a 10% reduction in compressional velocity can be achieved even with a fraction of a percent concentration of very thin cracks. Inclusions of larger aspect ratio, approaching a spherical shape, are less efficient at reducing velocity but for an aspect ratio of 0.1, only ~5% melt fraction would be required to achieve the reduction in velocities observed. It is not unreasonable to postulate that the regions flanking the small axial magma chamber contain a small, unconnected melt fraction which, from the HS bounds, will be electrically resistive. Either a distribution of very few extremely thin cracks or, a few percent of isolated inclusions of larger aspect ratio or, more likely, a combination of both, may result in a region in which p wave velocities are slightly reduced, while the electrical conductivity is not significantly increased.

The implications for this region seem to be that it is currently in a period of relative magmatic quiescence, in agreement with numerous other observations. This conclusion stems both from the nature of the uppermost extrusives and from the electrically resistive nature of the midcrust. If we assume that magmatism at ridges occurs as a cyclic process, then we can further infer that during the magmatically quiescent phase, the crust contains at most only a very small volume of melt. Most of the seismically determined LVZ must consist of a region in which melt, if present at all, is distributed in an unconnected texture of isolated pockets, veins or fractures and which is crystallizing in situ.

An important question is whether the crust beneath the EPR at 9°N, where volcanism is known to be occurring at present [*Haymon et al.*, 1991], and where there is good evidence of an AMZ [*Detrick et al.*, 1987; *Kent et al.*, 1990], would be shown by a CSEM experiment to be electrically conductive. If the AMZ is to be identified as such, then during periods of active magmatism, newly injected mantle derived melt must form an interconnected network throughout the mush zone. If, on the other hand, the melt within the LVZ fails to form an interconnected network, then a CSEM survey would return with similar results to those we have presented here. This situation could occur if the amount of melt present in the LVZ is always small, even during active periods, or the texture of the surrounding subsolidus gabbro does not allow a connected network to form. Thus CSEM experiments at other locations along the mid-ocean ridge system may be able to address the question of the degree to which the amount and texture of melt present within the crust at the axis is modulated by magmatic/tectonic cycles.

CONCLUSIONS

The section of the EPR near 13°N appears to be in a state of relatively subdued magmatic activity. The results of our CSEM survey indicate a generally resistive crust at all depths to around 2 km and negate the possibility of a large volume of high melt fraction beneath the ridge crest. The results are consistent with a picture of axial structure which contains at most a few percent partial melt, most of which is

in isolated crystallizing pockets, with a volumetrically small pool of slightly higher melt fraction (~10%) centered within 400 to 500 m beneath the ridge crest. It is possible that there are discrete pools of melt along axis, although our data are unable to resolve such small features.

Further CSEM experiments should be conducted in conjunction with or to supplement existing seismic refraction surveys over regions where there is good evidence for robust magma supplies. Such experiments may be used to identify whether the AMZ ever contains sufficient melt to form an interconnected texture throughout the large volume in the crust beneath the ridge crest. Other possibilities are that melt is supplied at a slower but steady rate from the mantle, or that even episodic melt injection from the mantle only results in small amounts of melt within the AMZ, below a small sill-like lens of higher melt fraction.

Acknowledgments. We would like to thank the captain and crew of the RRS *Charles Darwin* and all those who participated in cruise CD39/89. Special thanks are due to P. Patel, M. MacCormack, and J. Leonard, who were responsible for the Cambridge equipment and to C. Cox, S. Webb, and J. Lemire for the Scripps receivers. A. Chave is thanked for the use of his forward code and A. Flosadóttir for implementing the derivatives. We greatly appreciate the efforts of R.N. Edwards, A.G. Jones, and K. Rohr for their careful and thorough reviews, which greatly improved the structure of this paper. The project was supported by the NERC research grants GR3/5851 and GR3/6673. Two of us, R.L.E and M.J.U, received NERC studentships as well as support from colleges. The Scripps group was funded by NSF grant OCE88-22789.

REFERENCES

Browning, P., Cryptic variation within the cumulate sequence of the Oman ophiolite: Magma chamber depth and petrological implications, *Geol. Soc. Spec. Publ., 13*, 71-83, 1984.

Chave, A.D., Numerical integration of related Hankel transforms by quadrature and continued fraction expansion, *Geophysics, 48*, 1671-1686, 1983.

Chave, A.D., The Fréchet derivatives of electromagnetic induction, *J. Geophys. Res., 89*, 3373-3380, 1984.

Chave, A.D., and C.S. Cox, Controlled electromagnetic sources for measuring electrical conductivity beneath the oceans, 1, Forward problem and model study, *J. Geophys. Res., 87*, 5327-5338, 1982.

Chave, A.D., A. Flosadóttir, and C.S. Cox, Some comments on seabed propagation of ULF/ELF electromagnetic fields, *Radio Sci., 25*, 825-836, 1990.

Chave, A.D., S.C. Constable, and R.N. Edwards, Electrical exploration methods for the seafloor, in *Electromagnetic Methods in Applied Geophysics*, vol. II, edited by M.N. Nabighian, Society for Exploration Geophysicists, Tulsa, Okla., 1992.

Cheadle, M.J., Properties of texturally equilibrated two-phase aggregates, Ph.D. thesis, University of Cambridge, 1989.

Christeson, G.L., G.M. Purdy, and G.J. Fryer, Structure of young upper crust at the East Pacific Rise near 9°30'N, *Geophys. Res. Lett., 19*, 1045-1048, 1992.

Constable, S.C., Marine electromagnetic induction studies, *Geophysics, 11*, 303-327, 1990.

Constable, S.C., R.L. Parker, and C.G. Constable, Occam's inversion: A practical algorithm for generating smooth models from electromagnetic sounding data, *Geophysics, 52*, 289-300, 1987.

Cox, C.S., C.S. Constable, A.D. Chave, and S.C. Webb, Controlled source electromagnetic sounding of the oceanic lithosphere, *Nature, 320*, 52-54, 1986.

Detrick, R.S., P. Buhl, E. Vera, J. Orcutt, J. Madsen, and T. Brocher, Multi-channel seismic imaging of a crustal magma chamber along the East Pacific Rise, *Nature, 326*, 33-41, 1987.

Dick, H.J.B., P. Meyer, S. Bloomer, S. Kirby, D. Stakes, and C. Mawer, Lithostratigraphic evolution of an in situ section of oceanic layer 3, *Proc. Ocean Drill. Program Sci. Results, 118*, 439-515, 1991.

Evans, R.L., Electrical resistivity structure of the East Pacific Rise near 13°N, Ph.D. thesis, University of Cambridge, 1991.

Evans, R.L., S.C. Constable, M.C. Sinha, C.S. Cox, and M.J. Unsworth, Upper-crustal resistivity structure of the East Pacific Rise near 13°N, *Geophys. Res. Lett., 18*, 1917-1920, 1991.

Everett, M.E., and R.N. Edwards, Theoretical controlled-source electromagnetic responses of fast spreading mid-ocean ridge models, *Geophys. J. Int., 105*, 313-323, 1991.

Filloux, J., Instrumentation and experimental methods for oceanic studies, in *Geomagnetism 1*, edited by J.A. Jacobs, pp. 143-248, Academic, San Diego, Calif., 1987.

Harding, A.J., J.A. Orcutt, M.E. Kappus, E.E. Vera, J.C. Mutter, P. Buhl, R.S. Detrick, and T.M. Brocher, Structure of young oceanic crust at 13°N on the East Pacific Rise from expanding spread profiles, *J. Geophys. Res., 94*, 12,163-12,196, 1989.

Hashin, Z., and S. Shtrikman, A variational approach to the theory of effective magnetic permeability of multiphase materials, *J. Appl. Phys., 33*, 3125-3131, 1962.

Haymon, R.M., et al., Active eruption seen on East Pacfic Rise, *Trans. AGU, 72*, 505, 1991.

Kent, G.M., A.J. Harding, and J.A. Orcutt, Evidence for a smaller magma chamber beneath the East Pacific Rise at 9°30'N, *Nature, 344*, 650-653, 1990.

Kuster, G.T., and M.H. Toksoz, Velocity and attenuation of seismic waves in two phase media, 1, Theoretical formulations, *Geophysics, 39*, 587-606, 1974.

Langmuir, C.H., J.F. Bender, and R. Batiza, Petrological and tectonic segmentation of the East Pacific Rise, 5°30'N–14°30'N, *Nature, 322*, 422-429, 1986.

Madsen, J., R.S. Detrick, J.C. Mutter, P. Buhl, and J.A. Orcutt, A 2 and 3-D analysis of gravity anomalies associated with the East Pacific Rise at 9°N and 13°N, *J. Geophys. Res., 95*, 4967-4987, 1990.

Malpas, J , Crustal accretionary processes in the Troodos ophiolite, Cyprus: Evidence from field mapping and deep crustal drilling, in *Ophiolites. Oceanic crustal analogues. Proceedings of the Symposium Troodos 1987*, edited by J. Malpas et al., pp. 63-74, Geol. Surv. Dept., Nicosia, Cyprus. 1990.

Monti, S., P. Gente, J.P. Mazée, J.M. Auzende, H. Bougault, and K. Crane, Carte Bathymétrique de la Dorsale Est-Pacifique de 10°N à 14°30'N (Planche 7), *Inst. Français de Rech. pour l'Exploitation de la Mer*, Direction de L'Environnement et des Recherches Océaniques Departement des Géosciences Marines, Centre de Brest BP337, 29273 Brest, France, 1987.

Parker, R.L., The inverse problem of EM induction: Existence and construction of solutions based on incomplete data, *J. Geophys. Res., 85*, 4421-4428, 1980.

Parker, R.L., The inverse problem of electromagnetic sounding, *Geophysics, 49*, 2143-2158, 1984.

Schmeling, H., Numerical models on the influence of partial melt on elastic, anelastic and electrical properties of rocks, Part II, Electrical conductivity, *Phys. Earth Planet. Inter., 43*, 123-136, 1986.

Sinha, M.C., P.D. Patel, M.J. Unsworth, T.R.E. Owen, and M.R.G. MacCormack, An active source electromagnetic sounding system for marine use, *Mar. Geophys. Res., 12*, 59-68, 1990.

Sinton, J.M., and R.S. Detrick, Mid-ocean ridge magma chambers, *J. Geophys. Res., 97*, 197-216, 1992.

Smith, B.D., and S.H. Ward, On the computation of polarization ellipse parameters, *Geophysics, 39*, 867-869, 1974.

Unsworth, M.J., Electromagnetic exploration of the oceanic crust with a controlled source, Ph.D. thesis, University of Cambridge, 1991.

Unsworth, M.J., B.J. Travis, and A.D. Chave, Electromagnetic induction by a finite electric dipole source over a 2-D Earth, *Geophysics, 58*, 198-214, 1993.

Waff, H.S., and D.F. Weill, Electrical conductivity of magmatic liquids: Effects of temperature, oxygen fugacity and composition, *Earth Planet. Sci. Lett., 28*, 254-260, 1975.

Webb, S.C., S.C. Constable, C.S. Cox, and T.K. Deaton, A seafloor electromagnetic field instrument, *J. Geomagn. Geoelectr.*, *37*, 1115-1130, 1985.

Young, P.D. and C.S. Cox, Electromagnetic active source sounding near the East Pacific Rise, *Geophys. Res. Lett.*, *8*, 1043-1046, 1981.

S.C. Constable, Institute of Geophysics and Planetary Physics, Scripps Institution of Oceanography, La Jolla, Ca 92093.

R.L. Evans, Department of Physics, University Of Toronto, Toronto Ontario, M5S 1A7, Canada.

M.C. Sinha, Bullard Laboratories, Cambridge University, Cambridge CB3 OEZ, England.

M.J. Unsworth, Geophysics Program, AK-50, University of Washington, Seattle Wa 98195.

**(Received September 30, 1992;
revised July 6, 1993;
accepted July 7, 1993.)**